

RESEARCH

Open Access



Simultaneous and sensitive determination of ascorbic acid, dopamine and uric acid via an electrochemical sensor based on PVP-graphene composite

Yiyong Wu^{1,2†}, Peihong Deng^{2*}, Yaling Tian^{1,2†}, Jinxia Feng¹, Jingyun Xiao¹, Junhua Li², Jun Liu^{1†}, Guangli Li^{1†} and Quanguo He^{1,3*}

Abstract

A method with high sensitivity, good accuracy and fast response is of ever increasing importance for the simultaneous detection of AA, DA and UA. In this paper, a simple and sensitive electrochemical sensor, which based on the polyvinylpyrrolidone (PVP)-graphene composite film modified glassy carbon electrode (PVP-GR/GCE), was presented for detecting ascorbic acid (AA), dopamine (DA) and uric acid (UA) simultaneously. The PVP-GR/GCE has excellent electrocatalytic activity for the oxidation of AA, DA and UA. The second-order derivative linear sweep voltammetry was used for the electrochemical measurements. The peak potential differences of DA-AA, DA-UA, and UA-AA (measured on the PVP-GR/GCE) were 212, 130 and 342 mV respectively. Besides, the over potential of AA, DA and UA reduced obviously, so did the peak current increase. Under the optimum conditions, the linear ranges of AA, DA and UA were 4.0 μM –1.0 mM, 0.02–100 μM , and 0.04–100 μM , respectively. The detection limits were 0.8 μM , 0.002 μM and 0.02 μM for AA, DA, and UA. The electrochemical sensor presented the advantages of high sensitivity and selectivity, excellent reproducibility and long-term stability. Furthermore, the sensor was successfully applied to the analysis of real samples.

Keywords: Simultaneous determination, Polyvinylpyrrolidone, Ascorbic acid, Dopamine, Uric acid, Electrochemical sensor

Introduction

As the key small biomolecules in the physiological process of human metabolism, ascorbic acid (AA), dopamine (DA) and uric acid (UA) generally coexist in biological matrix at the same time. Abnormal levels of AA, DA

and UA will lead to some disorders and diseases, such as mental illness, Parkinson's disease, hyperuricemia and leukemia [1–4]. Therefore, it is of great significance to establish a sensitive and rapid method for the simultaneous detection of AA, DA and UA for the study of their physiological signal procession and diagnostic applications. However, since the signals of AA, DA and UA are overlap, it is difficult to obtain the content of these three compounds separately in the extracellular fluid of the central nervous system, and serum where they usually coexist.

For the determination of AA, DA and UA, several methods have been developed, such as using high performance liquid chromatography [5], chemiluminescence

*Correspondence: dph1975@163.com; hequanguo@126.com

[†]Yiyong Wu, Yaling Tian, Jun Liu and Guangli Li: same contribution

¹ School of Life Science and Chemistry, Hunan University of Technology, Zhuzhou 412007, China

² Key Laboratory of Functional Metal–Organic Compounds of Hunan Province; Key Laboratory of Functional Organometallic Materials of Hunan Provincial Universities, Department of Chemistry and Material Science, Hengyang Normal University, Hengyang 421008, China
Full list of author information is available at the end of the article



[6], capillary electrophoresis [7] and ultraviolet visible spectroscopy [8]. In recent years, electrochemical methods have been widely concerned because of their rapid response, high sensitivity, good stability, excellent selectivity and so on [9]. However, it's not able to determine the AA, DA and UA separately on bare electrode without any modifications since the oxidation potentials of these three compounds are approximate [10]. Recently, various materials have been used in electrode modification for overcoming this problem [11–13].

In recent years, various nanomaterials have been well applied in different fields [14]. Among them, graphene (GR) is a two-dimensional carbon nanomaterial composed of carbon atoms in a hexagonal lattice. It is a single-layer film of carbon atoms in hexagonal lattice. With the strengths of excellent conductivity, large specific surface area, wide potential window and low cost, it is considered as a potential nanomaterial for the design of new sensors [15–23]. However, the interaction between individual GR may not only lead to irreversible aggregation, but also even restock to form graphite, so that the dispersibility of GR in water and some other solvents is poor and the application is seriously limited. Thus, it is inadvisable to apply GR directly to simultaneous detection of small biomolecules. To address these issues, GR-based nanocomposites have been exploited in recent years to modify electrodes for simultaneously detecting the AA, DA and UA. For instance, Tukimin et al. were centered on using poly (3,4-ethylenedioxythiophene)/reduced graphene oxide/manganese dioxide composite as electrode material to construct electrochemical sensor for simultaneous detection of AA, DA and UA, with the detection limits as low as 1.00 μM , 0.02 μM , and 0.05 μM [24]. Besides, Tian et al. reported the detection of AA, DA and UA by gold nanoparticles/ β -cyclodextrin/graphene nanocomposite modified electrode (detection limits were 10 μM , 0.15 μM and 0.21 μM) [25]. Recently, Niu and his colleagues successfully proposed a sensor based on stacked graphene platelet nanofibers/ionic liquids/chitosan to test AA, DA and UA simultaneously [26]. Moreover, Sun's team used graphene/Pt nanocomposites as electrode modifiers for simultaneous determination of AA, DA and UA [27], and Lian et al. developed a new sensing platform based on tryptophan-functionalized GR modified electrode for detecting AA, DA and UA simultaneously [28]. In spite of the successful separation from the oxidation potentials of these three species by the above studies, some nanomaterials are relatively expensive, and some synthesis process is complex and time-consuming. Therefore, it is necessary to explore a preferable modified electrode which is easy to fabricated, cost-effective, and sensitive to achieve the simultaneous detection of these three substances.

Polyvinylpyrrolidone (PVP), as a kind of non-toxic polymer and non-ionic surfactant, exhibits ideal features for the electrode modification due to its strong adsorption capacity towards phenolic compounds due to the hydrogen bonding between imide moieties of polymer and hydroxyl group in phenolic compounds [29]. What's more, it was found that PVP was able to make the carbon atoms less prone to aggregation in GR nanosheets. Thus, the dispersion and stability of PVP-GR composite boosted obviously compared with pure GR. Herein, for the accurate detection of AA, DA and UA simultaneously on the same electrode, a simple detection method using PVP-GR/GCE was proposed. The sensor with good catalytic activity for the oxidation of AA, DA and UA could help to distinguish these three species with similar redox potentials. Furthermore, the electrochemical behaviors of AA, DA and UA at the PVP-GR/GCE were studied in detail.

Experimental

Chemicals and solutions

The solutions received from Sinopharm Chemical Reagent Co., Ltd. Graphite, polyvinylpyrrolidone, hydrazine solution (80 wt %), ammonia solution (25 wt %), hydrogen peroxide solution (30 wt %), ascorbic acid (AA), dopamine (DA) and uric acid (UA) were acquired from Aladdin Chemical Reagent Co., Ltd., China. Other reagents were analytical grade and adopted as received. All human urine samples were collected from the laboratory personnel. All aqueous solutions were prepared with ultra-pure water (specific resistance of 18 $\text{M}\Omega\text{ cm}$). 0.1 M phosphate buffered solutions (PBS, pH 6.0) was used throughout this study.

Instruments and characterizations

Cyclic voltammetry (CV) measurements were performed on a CHI 660E electrochemical workstation which was produced from Chenhua Instrument Co. Ltd. Shanghai, China. A model JP-303E polarographic analyzer from Chengdu Instrument Factory in China was used for quantitative analysis of the samples by the second-order derivative linear sweep voltammetry (SDLSV). The saturated calomel electrode (SCE), platinum wire electrode and modified glassy carbon electrode ($d=4\text{ mm}$) were used as the reference electrode, auxiliary electrode and working electrode respectively in this electrode system. The pH values were measured with a combined glass electrode on the pH-3c Model pH meter, which was purchased from Leichi Instrument Factory, Shanghai, China. Scanning electron microscope (EVO10, ZEISS, Jena, Germany) images were obtained under 2.0 kV accelerating voltage. A high-speed centrifuge (maximum speed

16000r/min) was provided by Changsha Yingtai Instrument Co., Ltd., China.

Preparations of GR and PVP-GR composite

First of all, the synthesis of graphite oxide was prepared by natural graphite powder [30, 31]. Secondly, 100 mg of graphite oxide was dissolved in ultra-pure water (100 mL) and exfoliated to be graphene oxide (GO) under sonication for 2 h to obtain a light yellow solution. Subsequently, centrifugation was performed to remove any impurities (usually in trace amount) adhered to graphite oxide. 10.0 mg PVP was added to a 20.0 mL GO solution, then stirred for 10 min at room temperature. Following on that, 20 μL hydrazine hydrate solution and 80 μL ammonia solution were added, and the mixture was reacted at 95° C for 1 h. At the end of the reaction, stable PVP-GR composite was obtained. As a control, the preparation method of GR was the same as above, except that no PVP was added.

Electrode preparation

Before modification, GCE was polished on a polishing cloth with 0.3 μm and 0.05 μm alumina slurries in sequence, then washed thoroughly with water between each polishing step. Subsequently, the GCE was sonicated with water and ethanol in turn. Finally, the GCE was dried under an infrared lamp. In order to prepare PVP-GR/GCE, PVP-GR dispersion (10 μL) was carefully dropped on the electrode surface and dried under an infrared lamp. Besides, PVP/GCE and GR/GCE were

also prepared by 10 μL of 1.0 mg mL^{-1} PVP and 10 μL of 1.0 mg mL^{-1} GR for comparison. The whole electrode preparation process was shown in Scheme 1.

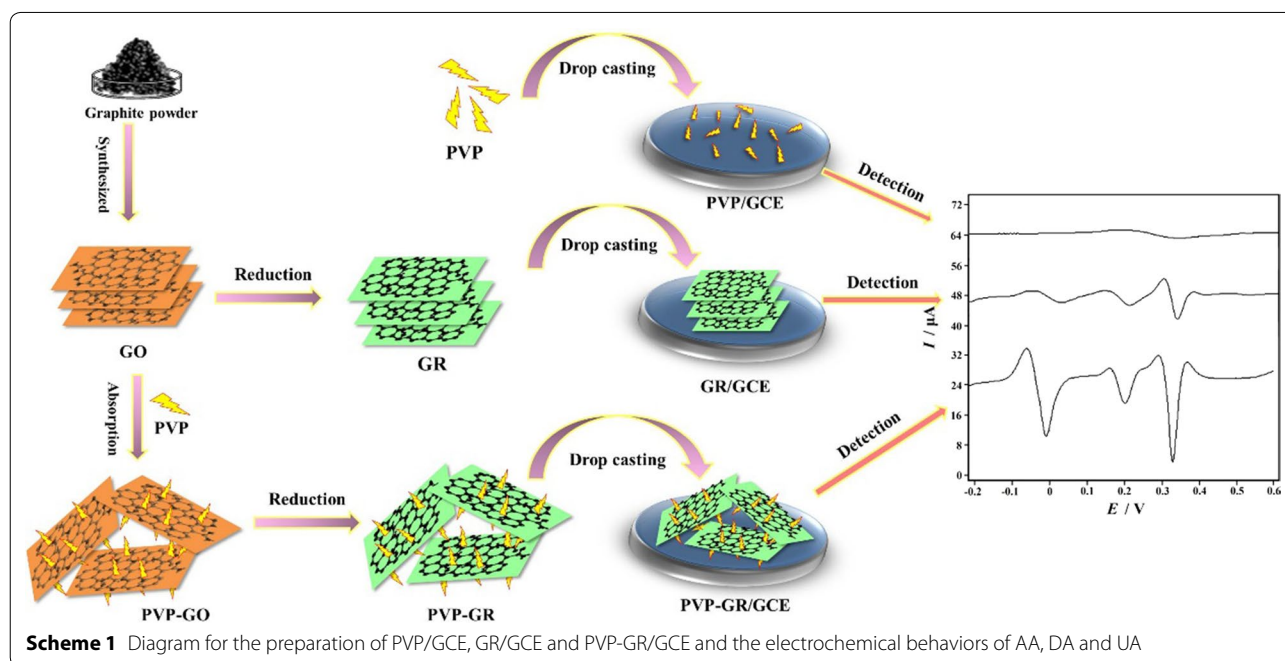
Electrochemical measurements

Electrochemical experiments were carried out by CV in a 10.0 mL 0.10 M PBS (pH 6.0) containing the single or mixed components of AA, DA and UA. The preconcentration of analytes was performed on the PVP-GR/GCE with an accumulation potential (0 V) under constant stirring. After a certain period of time, CV or SDLSV was performed in quiescent solution. For sample analysis, SDLSV was run with a positive going potential scan (−0.2–0.60 V) under optimal conditions. All the electrochemical measurements were carried out at room temperature without removing oxygen from the solution.

Results and discussion

SEM Characterizations of GR and PVP-GR

The surface morphology of GCE modified with GR and PVP-GR composite was investigated by SEM. It can be clearly observed the typically crumpled and wrinkled structure of GR in Fig. 1a. Figure 1b shows the SEM image of PVP-GR composite. The wrinkles on the GR sheets are clearly observed. This wrinkled nature of GR is highly beneficial in maintaining a high surface area on the electrode since the sheets cannot readily collapse back to a graphitic structure [32]. Most importantly, it could indicate that the dispersity of PVP-GR composite was much better, which was extremely essential for



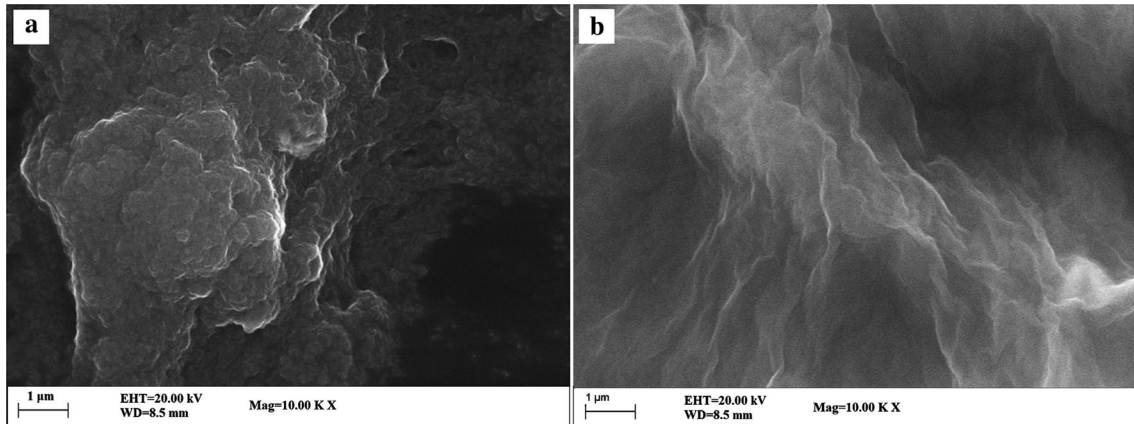


Fig. 1 SEM images of GR (a) and PVP-GR (b). Accelerating voltage: 20 kV

nanomaterials dispersed in solution and for their further application [33]. Therefore, it is greatly expected that the performance of the sensor is improved by the PVP-GR composite.

The element composition and distribution of PVP-GR nanocomposite were analyzed by EDS. As shown in Fig. 2, a series of peaks related to the species of C, O, and N were observed in the survey spectrum, which

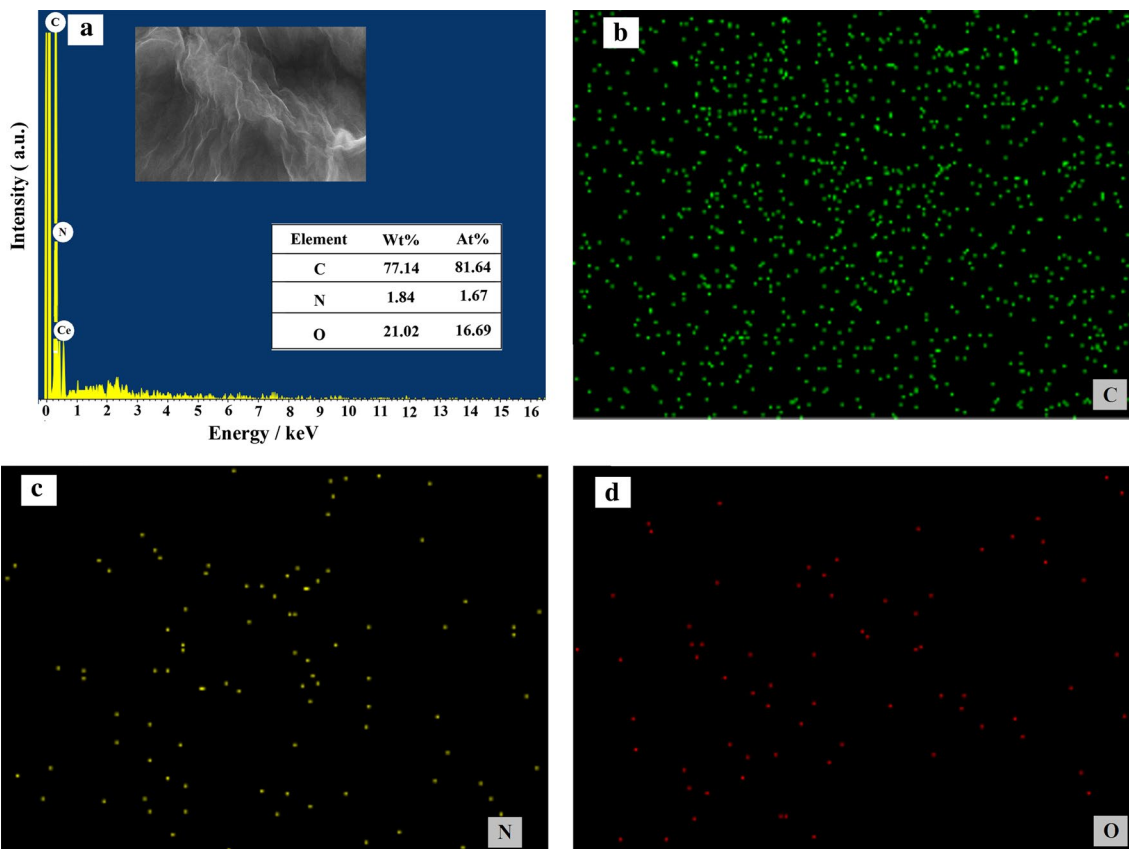


Fig. 2 EDS spectrum (a) and typical SEM image (insert of A) of PVP-GR nanocomposite together with the corresponding element mapping images of C (b), N (c) and O (d)

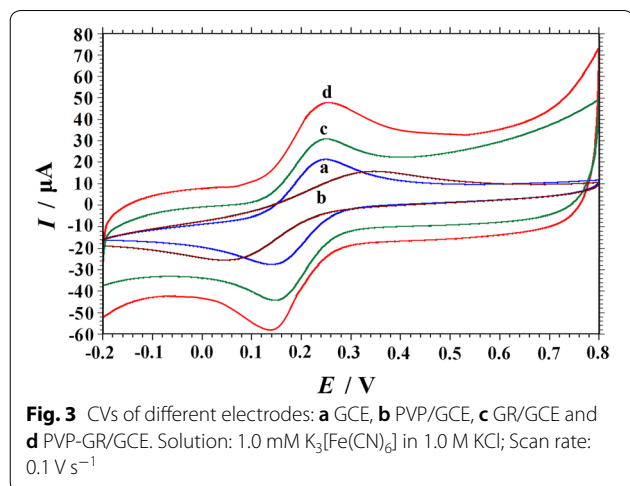
confirmed the presence of these chemical elements in the product. At the same time, the element mapping images (Fig. 2b–d) corresponding to the insert of Fig. 2a indicated that, C, O and N were uniformly dispersed on the nanocomposite, and C, O and N were present in the structure at 77.14, 21.02 and 1.84 wt % and 81.64, 16.69 and 1.67 At %, respectively.

Electrochemical characterization by CV

The electrochemical method was used to characterize the charge transfer characteristics of PVP-GR/GCE. The cyclic voltammograms (CVs) showed in Fig. 3 was obtained in 1.0 mM $K_3[Fe(CN)_6]$ solution containing 1.0 M KCl at bare GCE, PVP/GCE, GR/GCE and PVP-GR/GCE. Although the appearance of a pair of redox peaks showed on the electrodes, their potential differences (ΔE_p) were totally different. The potential difference of bare GCE (curve a), PVP/GCE (curve b), GR/GCE (curve c) and PVP-GR/GCE (curve d) was 109 mV, 298 mV, 103 mV and 105 mV, respectively. Apparently, a pair of well-defined quasi-reversible redox peaks appeared at the PVP-GR/GCE, and the peak current signal of PVP-GR/GCE was observably larger than the other three. According to Randles–Sevcik formula (1) [34]:

$$I_p = 2.69 \times 10^5 n^{3/2} A_{eff} D^{1/2} \nu^{1/2} C \quad (1)$$

where I_p is the peak current (A), n is the number of electrons transferred, A_{eff} is the effective area (cm^2), D is the diffusion coefficient of $K_3Fe(CN)_6$ ($7.6 \times 10^{-6} cm^2 s^{-1}$) [35], ν is the scan rate ($V s^{-1}$) and C corresponds to the bulk concentration of $K_3Fe(CN)_6$ ($mol cm^{-3}$). According to the above formula, the electroactive surface area of PVP-GR/GCE is calculated as $0.1996 cm^2$, which is larger than that of GR/GCE ($0.1493 cm^2$). The results released

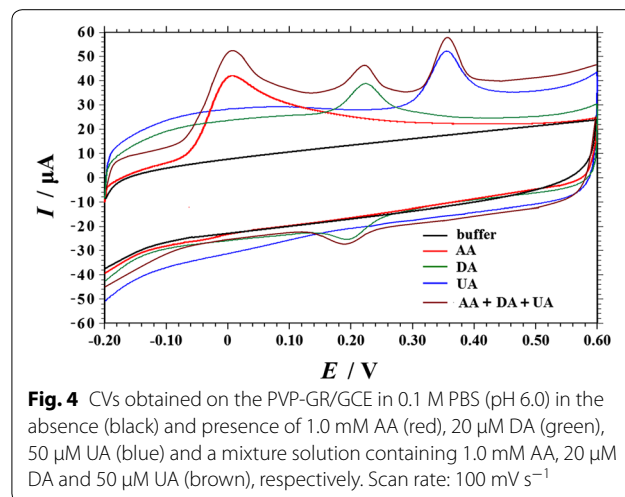


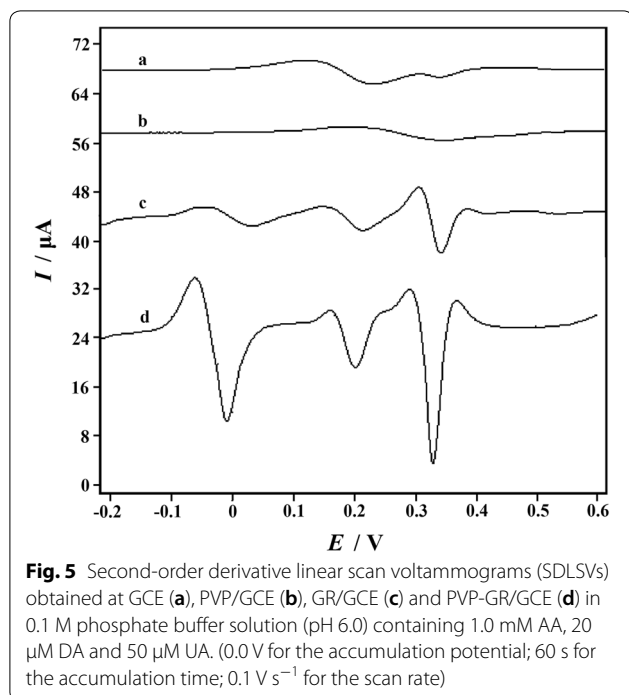
that the PVP-GR composite promoted the electron transfer rate, which may be contribute to the excellent conductivity and large specific surface area of PVP-GR modified on GCE surface.

Electrochemical behaviors of AA, DA and UA at PVP-GR/GCE

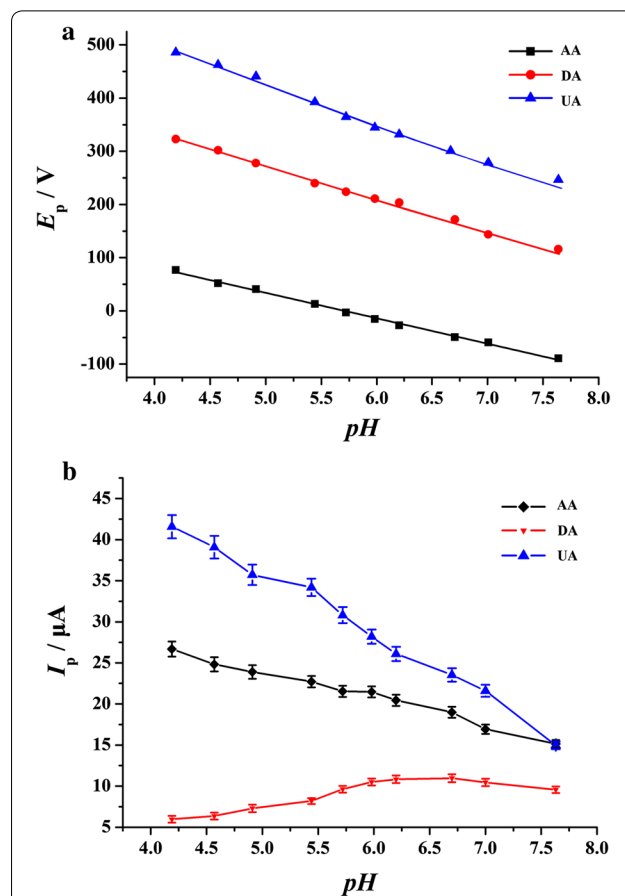
Figure 4 depicted the CV response in 0.1 M PBS (pH 6.0) obtained at the GR-PVP/GCE in the potential range of 0.0 to 1.2 V. As can be seen, no redox peaks were observed at the PVP-GR/GCE in the blank solution, indicating that the PVP-GR/GCE is non-electroactive in the selected potential region and there is no distribution of other reducing substances in the tested solution. The electrochemical behaviors of AA, DA, and UA at the PVP-GR/GCE were studied by CV in 0.1 M PBS (pH 6.0) containing AA, DA, UA and a mixture of AA, DA and UA respectively. In order to make the three substances have an obvious current response in the same range when determined simultaneously, 1.0 mM AA, 20 μM DA, and 50 μM UA were selected in our work. Figure 4 showed the irreversible electro-oxidation of AA and UA, while a reversible response of DA was exhibited at the PVP-GR/GCE. The $\Delta E_p = |E_{pa} - E_{pc}|$ is 29 mV and $I_{pa}/I_{pc} = 0.89$ for DA at $100 mV s^{-1}$. It can be detected in Fig. 4 that the anodic peaks of AA, DA and UA appeared approximately at the potential of 8, 194, and 356 mV, respectively. These data showed that it is feasible to discriminate these three species on the PVP-GR/GCE.

In order to demonstrate that the PVP-GR/GCE could simultaneously detect these three compounds, the SDLSV curves of the phosphate buffer solution (pH 6.0) with the simultaneous presence of 1.0 mM AA, 20 μM DA and 50 μM UA were also recorded. Figure 5 displayed the corresponding voltammetric curves of the mixture





obtained at bare GCE (curve a), PVP/GCE (curve b), GR/GCE (curve c) and PVP-GR/GCE (curve d) respectively. On the bare GCE, there are two peaks at 232 mV and 340 mV, corresponding to the overlapping voltammetric response of AA and DA and the oxidation of UA. The peak current is extremely weak ($I_p = 3.900 \mu A$ and $0.5125 \mu A$), which indicates that it is not feasible to detect these three small biomolecules simultaneously on bare GCE. At the PVP/GCE, it can be only observed a weak and broad peak at 0.35 V ($I_p = 1.938 \mu A$), which suggests that the oxidation peaks of that three may be not separated well. This is mainly due to the poor conductivity of PVP, which leads to the retardance of electron transfer. However, the oxidation peaks of AA, DA and UA presented at 34 mV ($I_p = 3.138 \mu A$), 214 mV ($I_p = 5.263 \mu A$), and 344 mV ($I_p = 9.325 \mu A$) on the GR/GCE, make it possible to detect these species simultaneously since GR has good catalytic ability for that three species. Three oxidation peak potentials of -10 mV (AA), 202 mV (DA) and 332 mV (UA) were obtained on the GR-PVP/GCE, which shifted negatively compared with GR/GCE. Distinctly, for GR-PVP/GCE, the peak currents increased significantly ($I_p = 20.21 \mu A$, $10.50 \mu A$ and $28.17 \mu A$). On one hand, with the good electrocatalytic activity and conductivity, GR could accelerate the electron transfer rate of AA, DA and UA on the electrode surface. On the other hand, it is well known that most unique properties are only associated with individual form. Therefore, preventing aggregation is particularly important for GR. The addition of PVP



can effectively prevent the aggregation of GR, so that the PVP-GR composite can be well dispersed in water. When it was modified on the GCE surface, it could effectively increase the GCE specific surface area. Therefore, the synergistic effect of PVP and GR significantly increased the peak signals of AA, DA and UA, and improved the sensitivity of the determination.

The effect of solution pH

It is well-known that the pH value of the analytical solution is of great significance to an experimental exploration, since the protons are involved in the electrode reactions. Therefore, the effects of pH value on the oxidation potential and current responses at PVP-GR/GCE were investigated in 1.0 mM AA, 20 μM DA and 50 μM UA, respectively. The acidity of the solution could affect the oxidation peak potential of AA, DA and UA. The result showed in Fig. 6a. With increasing the pH value, the oxidation potential of AA, DA and UA

shifted negatively. For AA, the linear regression equation was $E_{pa} \text{ (mV)} = 0.2726 - 0.04792 \text{ pH}$ ($R^2 = 0.9970$), while that one of DA was $E_{pa} \text{ (mV)} = 0.5760 - 0.06095 \text{ pH}$ ($R^2 = 0.9961$) and UA was $E_{pa} \text{ (mV)} = 0.7607 - 0.06785 \text{ pH}$ ($R^2 = 0.9829$). These results illustrated that electrochemical oxidation of AA, DA and UA followed Nernst equation, and the electrochemical reactions of them are all two-proton and two-electron transfer processes [36, 37]. At the same time, as shown in Fig. 6b, with the increase of solution pH value, the peak currents of AA and UA gradually reduced. However, on the contrary, the peak current of DA increased with the pH value reached to 6.0. However, the current of DA tended to decrease when the pH value was over 6.7. Thus, the larger peak current appeared at the pH value of 6.0–6.7. In order to determine these three substances sensitively at the same time, and considering the physiological pH value of 7.0, the pH value of 6.0 was selected for further study [38].

The effect of scan rate

Scan rate is one of the factors to study the electrochemical behavior. In this work, the electrochemical behavior of AA, DA and UA was further explored on the PVP-GR/GCE. Figure 7 showed the relationship between the scan rates and the currents of AA, DA and UA, respectively. In the range of 20–200 mV s^{-1} , the peak currents of the three compounds increased linearly with the scan rate. For AA (Fig. 7a) and UA (Fig. 7c), it is clearly observed that only one anodic peak presented in the voltammogram and the relationship between the peak current and the square root of scanning rate (Fig. 7a, c, inset). The linear regression equation of AA was $I_{pa} \text{ (}\mu\text{A)} = 4.9231 + 1.4961\nu^{1/2} \text{ ((mV s}^{-1}\text{)}^{1/2})$ ($R^2 = -0.9988$), and that one of UA was $I_{pa} \text{ (}\mu\text{A)} = -9.1577 + 3.9751\nu^{1/2} \text{ ((mV s}^{-1}\text{)}^{1/2})$ with a high correlation coefficient of $R^2 = -0.9992$. The results indicated that the diffusion controlled behavior dominated the electrode process of AA and UA. However, for DA (Fig. 7b), there were an anodic peak and a cathodic peak appeared in the CVs. Besides, the anodic and cathodic peak current of DA are linearly related to the scan rate (Fig. 7b, inset). The corresponding linear regression equations were $I_{pa} \text{ (}\mu\text{A)} = 1.919 + 0.0782\nu \text{ (mVs}^{-1}\text{)}$ ($R^2 = 0.9948$) and $I_{pc} \text{ (}\mu\text{A)} = 0.756 - 0.0921\nu \text{ (mV s}^{-1}\text{)}$ ($R^2 = 0.9955$), suggesting that the electrochemical oxidation of DA at PVP-GR/GCE was an absorption-controlled process. The fact might be attributed to the effective π - π conjugation between the aromatic moieties of DA and GR [39, 40].

Investigation of accumulation potential and accumulation time

Accumulation potential and accumulation time are also the important conditions for this work. The influence of

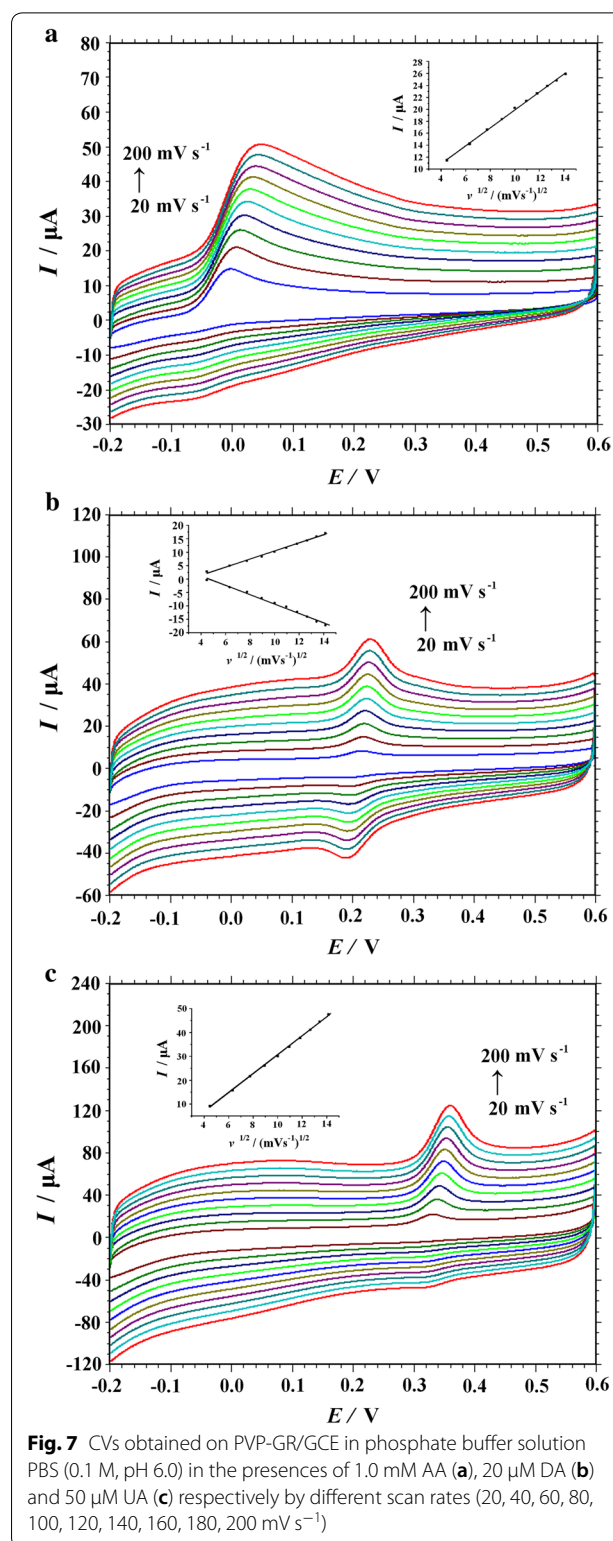
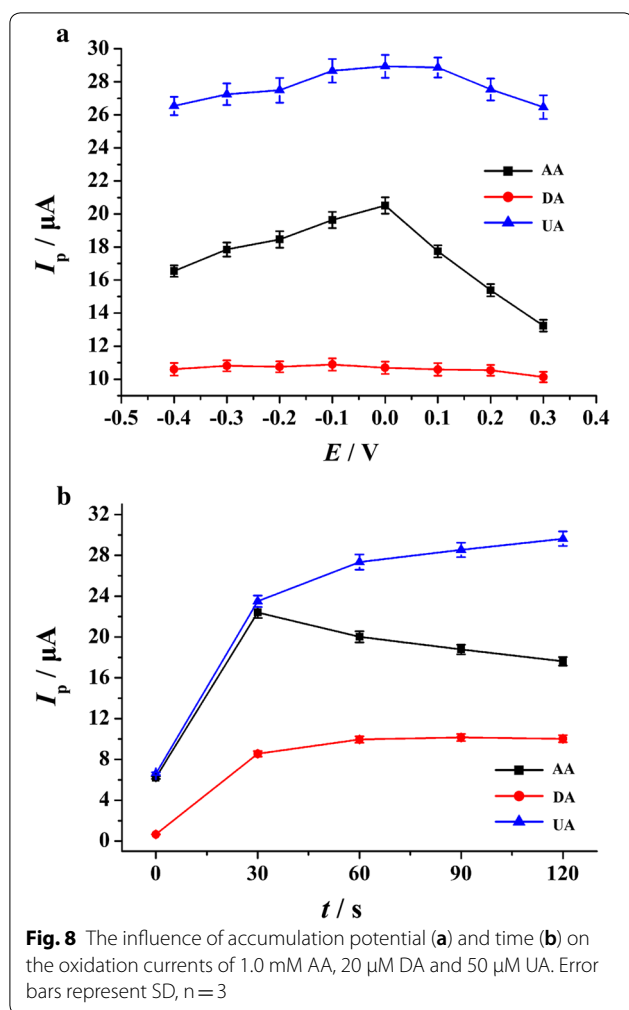


Fig. 7 CVs obtained on PVP-GR/GCE in phosphate buffer solution PBS (0.1 M, pH 6.0) in the presences of 1.0 mM AA (a), 20 μM DA (b) and 50 μM UA (c) respectively by different scan rates (20, 40, 60, 80, 100, 120, 140, 160, 180, 200 mV s^{-1})

accumulation potential and accumulation time on the peak currents of AA, DA and UA was studied by SDLSV. As the Fig. 8a presented, the peak currents of AA and UA



decreased slightly after increasing gradually as the potentials shifted from -0.40 to 0.30 V. However, the change of the peak current of DA was a little different in comparison, it was not affected by the accumulation potential. Therefore, according to the observation of the Fig. 8a, the accumulation potential of 0.0 V was considered to be beneficial to obtain the maximum peak currents for simultaneous detection of AA, DA and UA. In addition, time also made a difference on pre-concentration.

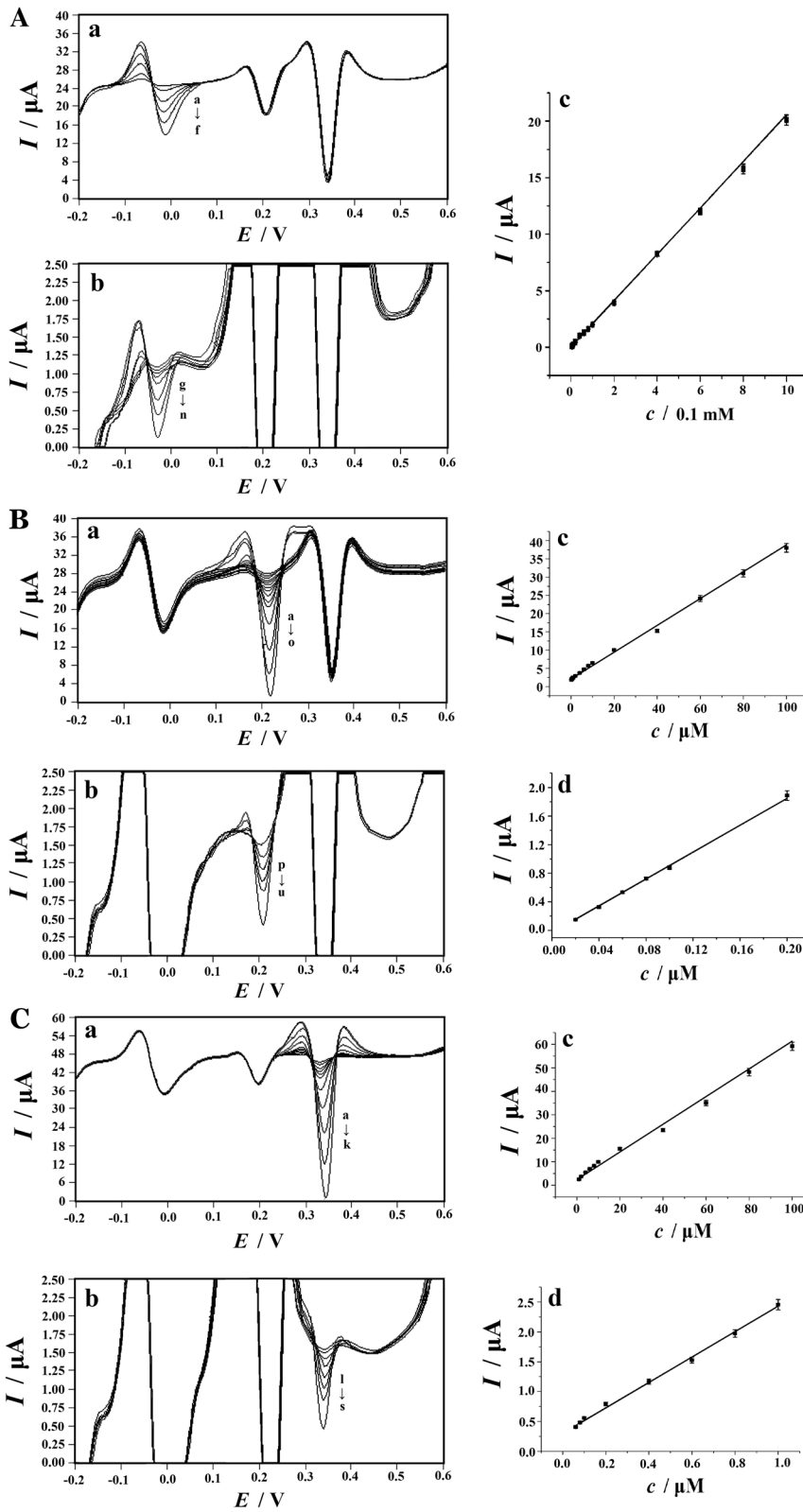
According to Fig. 8b, it could be described that the peak currents of AA, DA and UA increased rapidly with the increase of accumulation time. The maximum peak currents of AA, DA and UA were obtained at 30 s, 60 s and 90 s, respectively. For obtaining a stable peak with higher sensitivity and shorter analysis time, it was suggested that setting 60 s as the accumulation time to detect AA, DA, and UA is optimum.

Simultaneous determination of DA, AA and UA

Compared with CV, SDLSV has higher current sensitivity and better resolution, it was a good electrochemical technique for the simultaneous detection of AA, DA and UA. Under the optimized conditions, the potential range of -0.2 V to 0.6 V was selected for the measurements. When the concentration of one substance changed, the concentrations of the other two substances remained unchanged. It can be obviously described that the current response of the target molecules (AA, DA, or UA) enhanced linearly with the increasing of the corresponding target molecules concentration. According to Fig. 9, when the concentration range of AA was 4.0 μ M -1.0 mM with the presence of 20 μ M DA and 50 μ M UA, the electrochemical response of AA grew linearly as the concentration of AA increased (Fig. 9A). I_{pa} (μ A) = $0.00726 + 0.02054c$ (μ M) ($R = 0.9891$) was the regression equation of AA. Besides, as shown in Fig. 9B, the oxidation peak currents of DA were obtained in various concentration of DA (0.02 – 0.2 μ M and 0.2 – 100 μ M), with the presence of 1.0 mM AA and 50 μ M UA. A positive correlation between the increase in DA concentration and the increase of current response of DA was found. The regression equations were I_{pa} (μ A) = $0.040 + 9.4239c$ (μ M) ($R = 0.9985$) and I_{pa} (μ A) = $2.0587 + 0.3685c$ (μ M) ($R = 0.9828$). Similarly, it was revealed in Fig. 9C that the signal of UA increased linearly with increasing the concentration of UA from 0.04 – 1.0 μ M and 1.0 – 100 μ M, while the concentrations of AA and DA was 1.0 mM and 20 μ M in the analytical solutions. The regression equation were I_{pa} (μ A) = $0.3083 + 2.1242c$ (μ M) with a high correlation coefficient of $R = 0.9901$, and I_{pa} (μ A) = $2.3954 + 0.5897c$ (μ M) ($R = 0.9669$) with the detection limit of 0.02 μ M. The limit of detection (LOD)

(See figure on next page.)

Fig. 9 **A** SDLSVs of AA at the PVP-GR/GCE in the presence of 20 μ M DA and 50 μ M UA. a AA concentrations (from a to f): 100 , 200 , 400 , 600 , 80 , 1000 μ M; b AA concentrations (from g to n): 4 , 6 , 8 , 10 , 20 , 40 , 60 , 80 μ M. c Plots of peak height vs. AA concentration in the range of 4 – 1000 μ M. **B** SDLSVs of DA at the PVP-GR/GCE in the presence of 1.0 mM AA and 50 μ M UA. a DA concentrations (from a to o): 0.2 , 0.4 , 0.6 , 0.8 , 1.0 , 2.0 , 4.0 , 6.0 , 8.0 , 10 , 20 , 40 , 60 , 80 and 100 μ M; b DA concentrations (from p to u): 0.02 , 0.04 , 0.06 , 0.08 , 0.1 , 0.2 μ M; c Plots of peak height vs. DA concentration in the range of 0.2 – 100 μ M and d in the range of 0.02 – 0.2 μ M. **C** SDLSVs of UA at the PVP-GR/GCE in the presence of 1.0 mM AA and 20 μ M DA. a UA concentrations (from a to k): 1.0 , 2.0 , 4.0 , 6.0 , 8.0 , 10 , 20 , 40 , 60 , 80 , and 100 μ M; b UA concentrations (from l to s): 0.04 , 0.06 , 0.08 , 0.1 , 0.2 , 0.4 , 0.6 , 0.8 μ M; c Plots of peak height vs. UA concentration in the range of 1.0 – 100 μ M and d in the range of 0.04 – 1.0 μ M. 0.1 M PBS (pH 6.0) for the supporting electrolyte, 0.0 V for the accumulation potential, 60 s for the accumulation time, 0.1 V s^{-1} for the scan rate. Error bars represent SD, n = 3



was calculated by using IUPAC (International Union of Pure and Applied Chemistry) definitions, using the following equation:

$$LOD = 3s/m.$$

where *s* is the standard deviation of the blank signal, and *m* was the slope of the calibration straight line in the low concentration range. The SD of blank sample for AA, DA and UA were 0.0005460, 0.0006434 and 0.01315, respectively. The slopes of the calibration straight line in the low concentration range for AA, DA, UA were 0.02054 μA/μM, 9.4239 μA/μM, 2.1242 μA/μM, respectively. Therefore, the LOD of AA, DA and UA was calculated to be 0.8 μM, 0.002 μM and 0.02 μM, respectively.

The results by this method were compared with those in the literature (Table 1). By contrast, it can be easily found that lower detection limit, higher sensitivity and wider linear range were obtained at PVP-GR/GCE.

Reproducibility, repeatability and stability of the modified electrode

Reproducibility, repeatability and stability all played important roles in evaluating the accuracy of the proposed method. Ten equally prepared electrodes were tested in the mixture solution of 1.0 mM AA, 20 μM DA and 50 μM UA, to evaluate the reproducibility of the

PVP-GR/GCE by SDLSV. The relative standard deviations (RSD) of the peak currents of AA, DA and UA were 4.8%, 5.7% and 4.2% respectively. Moreover, the repeatability was obtained in the above mixture solution at a single PVP-GR/GCE for seven successive measurements. The RSD values of AA, DA and UA were 2.3%, 3.4% and 2.8%. These results indicated that the reproducibility and repeatability of PVP-GR/GCE was acceptable. When the PVP-GR/GCE was not in use, it was stored in air at 4 °C. The stability of the PVP-GR/GCE was studied in 7 days and 15 days respectively. There was no significant change after 7 days storage, and the current maintained 95.4% of the initial current. After 15 days of storage, the current also remained 83.6% compared with the initial current. The results showed that the stability of PVP-GR/GCE was decent.

Analytical applications

For the evolution of the applicability of the proposed method, AA, DA and UA in human urine samples were analyzed at the PVP-GR/GCE. The samples were diluted 100 times with phosphate buffer solution, and then 1 mL of the diluted urine samples were transferred to a voltammetric cell, and analyzed according to the above-described procedure. The test results were shown in Table 2. No signals of AA and DA were observed while the UA concentrations were 1.58~3.16 μM. Considered

Table 1 Comparison of analytical performance of PVP-GR/GCE with other modified electrodes in the literature

Modified electrode	Technique	Linear range/μM			Detection limit/μM			Reference
		AA	DA	UA	AA	DA	UA	
Pd/CNF-CPE ^a	DPV ⁱ	50–4000	0.5–160	2.0–200	15.0	0.20	0.70	[11]
PGE-DA ^b	DPV	25–500	1.0–20	2.5–30	13.0	0.11	1.40	[12]
MCNT/CCE ^c	DPV	15–800	0.5–100	0.55–90	7.71	0.31	0.42	[13]
PrGO/MnO ₂ /CCE ^d	DPV	1–800	0.03–45	0.3–80	1.00	0.02	0.05	[20]
AuNPs-β-CD-GR/GCE ^e	SWV ^j	30–2000	0.50–150	0.5–60	10	0.15	0.21	[21]
SGNF/IL/CS/GCE ^f	DPV	30–350	0.05–240	0.12–260	14.8	0.04	0.10	[22]
GR-Pt/GCE ^g	Amperometry	0.15–34.4	0.03–8.13	0.05–11.85	0.15	0.03	0.05	[23]
Trp-GR/GCE ^h	DPV	200–12900	0.5–110	10–1000	10.09	0.29	1.24	[24]
PVP-GR/GCE	SDLSV	4.0–1000	0.02–0.2; 0.2–100	0.04–1.0; 1.0–100	0.8	0.002	0.02	This work

^a Palladium nanoparticle-loaded carbon nanofibers modified carbon paste electrode

^b Pyrolytic graphite electrode modified into dopamine solution

^c MWCNT modified carbon-ceramic electrode

^d Poly(3,4-ethylenedioxythiophene)/reduced graphene oxide/manganese dioxide modified glassy carbon electrode

^e Gold nanoparticles-β-cyclodextrin-graphene-modified electrode

^f Stacked graphene platelet nanofibers/ionic liquids/chitosan modified glassy carbon electrode

^g Graphene/size-selected Pt nanocomposites modified glassy carbon electrode

^h Tryptophan functionalized graphene modified glassy carbon electrode

ⁱ Differential pulse voltammetry

^j Square wave voltammetry

Table 2 Determination of AA, DA, and UA in human urine samples (n = 4)

Samples ^a	Detected ^a /μM			Added/μM			Found ^b /μM			Recovery/%		
	AA	DA	UA	AA	DA	UA	AA	DA	UA	AA	DA	UA
Urine 1	–	–	2.57 (±0.09)	10.0	10.0	2.0	10.25 (±0.42)	10.18 (±0.37)	4.63 (±0.19)	102.5	101.8	103.0
Urine 2	–	–	1.58 (±0.08)	50.0	5.0	1.0	48.67 (±1.86)	5.27 (±0.26)	2.56 (±0.10)	97.3	105.4	98.0
Urine 3	–	–	3.16 (±0.14)	20.0	2.0	3.0	20.36 (±0.94)	2.07 (±0.09)	6.09 (±0.28)	101.8	103.5	97.7

^a All human urine samples were collected from the laboratory personnel

^b Average ± confidence interval, the confidence level is 95%

the dilution of the samples, the UA contents in the urine samples were calculated to be 1.58~3.16 mM. Standard AA, DA and UA solutions were added to the sample solution for recovery test. The results showed that the recoveries of AA, DA and UA were 97.3%–102.5%, 101.8%–105.4% and 97.7%–103.0% respectively. Acceptably and satisfyingly, these results indicated this developed method were validated and reliable. Additionally, the results also showed that AA, DA and UA can be determined by this method individually or simultaneously without interference.

Conclusion

In this paper, PVP-GR composite was prepared and exhibited good dispersibility and film-forming properties. A uniform and stable film can be formed on the GCE surface by a simple drop-coating method. The electrochemical behavior of AA, DA and UA on PVP-GR/GCE was explored by cyclic voltammetry. Moreover, with the unique structure of the modified layer and the synergistic effect of GR and PVP, the modified electrode had good catalytic activity for the electrochemical oxidation of AA, DA and UA. Besides, the three peaks could be clearly separated, which can achieve the simultaneous determination of the three small biomolecules. Most importantly, the PVP-GR/GCE was applied to the determination of AA, DA and UA in human urine samples with satisfactory results. The developed methodology was successfully adopted to the simultaneous analysis of these species in human metabolism during early stage of diseases, and also provided a promising strategy in this field. Therefore, it should have a good development prospect.

Acknowledgements

We sincerely express our thanks to all participants who offered urine samples for this study.

Authors' contributions

PD and QH conceived and designed the experiments; YW, YT, JF and JX performed the experiments; YW and JL analyzed the data; GL and QH contributed reagents/materials/analysis tools; QH and PD wrote the paper. All authors read and approved the final manuscript.

Funding

This work was supported by the key Project of Department of Education of Guangdong Province (2016GCZX008), the Project of Foshan Engineering Research Centre (20172010018), Key Disciplines' Construction Opening Fund of Foshan University (CGS06021), the Research and Innovation Project for Postgraduates of the Hunan Province Education Department (CX20190854), Scientific Research Fund of Hunan Provincial Education Department (18A336), Doctoral Program Construction of Hunan University of Technology, the NSFC (61703152), the Project of Science and Technology of Hunan Province Education Department (18A273, 18C0522), the Provincial Natural Science Foundation of Hunan (2020JJ4149, 2016JJ4010, 2018JJ34).

Availability of data and materials

All data and materials are fully available without restriction.

Ethics approval and consent to participate

The authors declare that all individual participants from whom the urine samples were obtained gave informed consent, and the studies have been approved by the Hunan University of Technology Ethics Committee and have been performed in accordance with ethical standards.

Consent for publication

Written informed consent for publication was obtained from all participants.

Competing interests

The authors declare that they have no competing interests.

Author details

¹ School of Life Science and Chemistry, Hunan University of Technology, Zhuzhou 412007, China. ² Key Laboratory of Functional Metal–Organic Compounds of Hunan Province; Key Laboratory of Functional Organometallic Materials of Hunan Provincial Universities, Department of Chemistry and Material Science, Hengyang Normal University, Hengyang 421008, China. ³ School of Materials Science and Energy Engineering, Foshan University, Foshan 528000, China.

Received: 6 March 2020 Accepted: 5 August 2020

Published online: 10 August 2020

References

- Liu Y, Huang J, Hou H, You T. Simultaneous determination of dopamine, ascorbic acid and uric acid with electrospun carbon nanofibers modified electrode. *Electrochem Commun.* 2008;10:1431–4. <https://doi.org/10.1016/j.elecom.2008.07.020>.
- Wu L, Feng LY, Ren JS, Qu XG. Electrochemical detection of dopamine using porphyrin-functionalized graphene. *Biosens Bioelectron.* 2012;34:57–62. <https://doi.org/10.1016/j.bios.2012.01.007>.
- Huang SH, Liao HH, Chen DH. Simultaneous determination of norepinephrine, uric acid, and ascorbic acid at a screen printed carbon electrode modified with polyacrylic acid-coated multi-wall carbon nanotubes. *Biosens Bioelectron.* 2010;25:2351–5. <https://doi.org/10.1016/j.bios.2010.03.028>.

4. Lakshmi D, Whitcombe MJ, Davis F, Sharma PS, Prasad BB. Electrochemical detection of uric acid in mixed and clinical samples: A review. *Electroanalysis*. 2011;23:305–20. <https://doi.org/10.1002/elan.201000525>.
5. Hubbard KE, Wells A, Owens TS, Tagen M, Fraga CH, Stewart CF. Determination of dopamine, serotonin, and their metabolites in pediatric cerebrospinal fluid by isocratic high performance liquid chromatography coupled with electrochemical detection. *Biomed Chromatogr*. 2010;24:626–31. <https://doi.org/10.1002/bmc.1338>.
6. Chen H, Li R, Lin L, Guo G, Lin J. Determination of L-ascorbic acid in human serum by chemiluminescence based on hydrogen peroxide–sodium hydrogen carbonate–CdSe/CdS quantum dots system. *Talanta*. 2010;81:1688–96. <https://doi.org/10.1016/j.talanta.2010.03.024>.
7. Szantai E, Szilagyi A, Guttman A, Sasvari-Szekely M, Ronai Z. Genotyping and haplotyping of the dopamine D4 receptor gene by capillary electrophoresis. *J Chromatogr A*. 2004;1053:241–5. <https://doi.org/10.1016/j.chroma.2004.04.012>.
8. Fraisse L, Bonnet MC, de Farcy JP, Agut C, Dersigny D, Bayol A. A colorimetric 96-well microtiter plate assay for the determination of urate oxidase activity and its kinetic parameters. *Anal Biochem*. 2002;309:173–9. [https://doi.org/10.1016/S0003-2697\(02\)00293-2](https://doi.org/10.1016/S0003-2697(02)00293-2).
9. Wu Y, Deng P, Tian Y, Ding Z, Li G, Liu J, Zuberi Z, He Q. Rapid recognition and determination of tryptophan by carbon nanotubes and molecularly imprinted polymer-modified glassy carbon electrode. *Bioelectrochemistry*. 2020. <https://doi.org/10.1016/j.bioelechem.2019.107393>.
10. Doménech A, García H, Doménech-Carbó MT, Galletero MS. 2,4,6-Triphenylpyrylium ion encapsulated into zeolite Y as a selective electrode for the electrochemical determination of dopamine in the presence of ascorbic acid. *Anal Chem*. 2002;74:562–9. <https://doi.org/10.1021/ac101657i>.
11. Huang J, Liu Y, Hou H, You T. Simultaneous electrochemical determination of dopamine, uric acid and ascorbic acid using palladium nanoparticle-loaded carbon nanofibers modified electrode. *Biosens Bioelectron*. 2008;24:632–7. <https://doi.org/10.1016/j.bios.2008.06.011>.
12. da Silva RP, Lima AWO, Serrano SHP. Simultaneous voltammetric detection of ascorbic acid, dopamine and uric acid using a pyrolytic graphite electrode modified into dopamine solution. *Anal Chim Acta*. 2008;612:89–98. <https://doi.org/10.1016/j.aca.2008.02.017>.
13. Habibi B, Pournaghi-Azar MH. Simultaneous determination of ascorbic acid, dopamine and uric acid by use of a MWCNT modified carbon-ceramic electrode and differential pulse voltammetry. *Electrochim Acta*. 2010;55:5492–8. <https://doi.org/10.1016/j.electacta.2010.04.052>.
14. He Q, Liu J, Liang J, Liu X, Li W, Liu Z, Ding Z, Tuo D. Towards improvements for penetrating the blood-brain barrier—recent progress from a material and pharmaceutical perspective. *Cells*. 2018;7:24. <https://doi.org/10.3390/cells7040024>.
15. He Q, Tian Y, Wu Y, Liu J, Li G, Deng P, Chen D. Facile and ultrasensitive determination of 4-nitrophenol based on acetylene black paste and graphene hybrid electrode. *Nanomaterials*. 2019;9:429. <https://doi.org/10.3390/nano9030429>.
16. He Q, Wu Y, Tian Y, Li G, Liu J, Deng P, Chen D. Facile electrochemical sensor for nanomolar rutin detection based on magnetite nanoparticles and reduced graphene oxide decorated electrode. *Nanomaterials*. 2019;9:115. <https://doi.org/10.3390/nano9010115>.
17. Ding Z, Deng P, Wu Y, Tian Y, Li G, Liu J, He Q. A novel modified electrode for detection of the food colorant sunset yellow based on nanohybrid of MnO₂ nanorods-decorated electrochemically reduced graphene oxide. *Molecules*. 2019;24:1178. <https://doi.org/10.3390/molecules24061178>.
18. Wu Y, Deng P, Tian Y, Magesa F, He Q. Construction of effective electrochemical sensor for the determination of quinalone yellow based on different morphologies of manganese dioxide functionalized graphene. *J Food Compos Anal*. 2019;84:103280. <https://doi.org/10.1016/j.jfca.2019.103280>.
19. He Q, Liu J, Liu X, Li G, Chen D, Deng P, Liang J. A promising sensing platform toward dopamine using MnO₂ nanowires/electro-reduced graphene oxide composites. *Electrochim Acta*. 2019;296:683–92. <https://doi.org/10.1016/j.electacta.2018.11.096>.
20. He Q, Liu J, Liu X, Li G, Deng P, Liang J. Preparation of Cu₂O-reduced graphene nanocomposite modified electrodes towards ultrasensitive dopamine detection. *Sensors*. 2018;18:199. <https://doi.org/10.3390/s18010199>.
21. He Q, Liu J, Liu X, Li G, Deng P, Liang J. Manganese dioxide Nanorods/ electrochemically reduced graphene oxide nanocomposites modified electrodes for cost-effective and ultrasensitive detection of Amaranth. *Colloids Surf, B*. 2018;172:565–72. <https://doi.org/10.1016/j.colsurfb.2018.09.005>.
22. He Q, Liu J, Liu X, Li G, Chen D, Deng P, Liang J. Fabrication of amine-modified magnetite-electrochemically reduced graphene oxide nanocomposite modified glassy carbon electrode for sensitive dopamine determination. *Nanomaterials*. 2018;8:194. <https://doi.org/10.3390/nano8040194>.
23. Tian Y, Deng P, Wu Y, Li J, Liu J, Li G, He Q. MnO₂ nanowires-decorated reduced graphene oxide modified glassy carbon electrode for sensitive determination of bisphenol a. *J Electrochem Soc*. 2020. <https://doi.org/10.1149/1945-7111/ab79a7>.
24. Tukimin N, Abdullah J, Sulaiman Y. Electrodeposition of poly(3,4-ethylene-dioxythiophene)/reduced graphene oxide/manganese dioxide for simultaneous detection of uric acid, dopamine and ascorbic acid. *J Electroanal Chem*. 2018;820:74–81. <https://doi.org/10.1016/j.jelechem.2018.04.065>.
25. Tian X, Cheng C, Yuan H, Du J, Xiao D, Xie S, Choi MMF. Simultaneous determination of L-ascorbic acid, dopamine and uric acid with gold nanoparticles-β-cyclodextrin-graphene-modified electrode by square wave voltammetry. *Talanta*. 2012;93:79–85. <https://doi.org/10.1016/j.talanta.2012.01.047>.
26. Niu X, Yang W, Guo H, Ren J, Yang F, Gao J. A novel and simple strategy for simultaneous determination of dopamine, uric acid and ascorbic acid based on the stacked graphene platelet nanofibers/ionic liquids/chitosan modified electrode. *Talanta*. 2012;99:984–8. <https://doi.org/10.1016/j.talanta.2012.07.077>.
27. Sun CL, Lee HH, Yang JM, Wu CC. The simultaneous electrochemical detection of ascorbic acid, dopamine, and uric acid using graphene/size-selected Pt nanocomposites. *Biosens Bioelectron*. 2011;26:3450–5. <https://doi.org/10.1016/j.bios.2011.01.023>.
28. Lian Q, He Z, He Q, Luo A, Yan K, Zhang D, Lu X, Zhou X. Simultaneous determination of ascorbic acid, dopamine and uric acid based on tryptophan functionalized graphene. *Anal Chim Acta*. 2014;823:32–9. <https://doi.org/10.1016/j.aca.2014.03.032>.
29. Yang C, Zhao J, Xu J, Hu C, Hu S. A highly sensitive electrochemical method for the determination of Sudan I at polyvinylpyrrolidone modified acetylene black paste electrode based on enhancement effect of sodium dodecyl sulphate. *Int J Environ Anal Chem*. 2009;89:233–44. <https://doi.org/10.1080/03067310802688579>.
30. He Q, Liu J, Tian Y, Wu Y, Magesa F, Deng P, Li G. Facile preparation of Cu₂O nanoparticles and reduced graphene oxide nanocomposite for electrochemical sensing of Rhodamine B. *Nanomaterials*. 2019;9:958. <https://doi.org/10.3390/nano9070958>.
31. He Q, Liu J, Xia Y, Tuo D, Deng P, Tian Y, Wu Y, Li G, Chen D. Rapid and sensitive voltammetric detection of rhodamine B in chili-containing foodstuffs using MnO₂ nanorods/electro reduced graphene oxide composite. *J Electrochem Soc*. 2019. <https://doi.org/10.1149/2.1271910jes>.
32. Deng P, Xu Z, Zeng R, Ding C. Electrochemical behavior and voltammetric determination of vanillin based on an acetylene black paste electrode modified with graphene–polyvinylpyrrolidone composite film. *Food Chem*. 2015;180:156–63. <https://doi.org/10.1016/j.foodchem.2015.02.035>.
33. He Q, Tian Y, Wu Y, Liu J, Li G, Deng P, Chen D. Electrochemical sensor for rapid and sensitive detection of tryptophan by a Cu₂O nanoparticles coated reduced graphene oxide nanocomposite. *Biomolecules*. 2019;9:176. <https://doi.org/10.3390/biom9050176>.
34. Bard AJ, Faulkner LR. *Electrochemical Methods*. 2nd ed. New York: Wiley; 2001.
35. Gooding JJ, Praig VG, Hall EAH. Platinum-catalyzed enzyme electrodes immobilized on gold using self-assembled layers. *Anal Chem*. 1998;70:2396–402.
36. Hu G, Ma Y, Guo Y, Shao S. Electrocatalytic oxidation and simultaneous determination of uric acid and ascorbic acid on the gold nanoparticles-modified glassy carbon electrode. *Electrochim Acta*. 2008;53:6610–5. <https://doi.org/10.1016/j.electacta.2008.04.054>.
37. Zhao Y, Gao Y, Zhan D, Liu H, Zhao Q, Kou Y, Shao Y, Li M, Zhuang Q, Zhu Z. Selective detection of dopamine in the presence of ascorbic acid and uric acid by a carbon nanotubes-ionic liquid gel modified electrode. *Talanta*. 2005;66:51–7. <https://doi.org/10.1016/j.talanta.2004.09.019>.

38. Temocin Z. Modification of glassy carbon electrode in basic medium by electrochemical treatment for simultaneous determination of dopamine, ascorbic acid and uric acid. *Sensors Actuators Chem.* 2013;176:796–802. <https://doi.org/10.1016/j.snb.2012.09.078>.
39. Li SJ, He JZ, Zhang MJ, Zhang RX, Lv XL, Li SH, Pang H. Electrochemical detection of dopamine using water-soluble sulfonated graphene. *Electrochim Acta.* 2013;102:58–65. <https://doi.org/10.1016/j.electacta.2013.03.176>.
40. Raj MA, John SA. Fabrication of electrochemically reduced graphene oxide films on glassy carbon electrode by self-assembly method and

their electrocatalytic application. *J Phys Chem C.* 2013;117:4326–35. <https://doi.org/10.1021/jp400066z>.

Publisher's Note

Springer Nature remains neutral with regard to jurisdictional claims in published maps and institutional affiliations.

Ready to submit your research? Choose BMC and benefit from:

- fast, convenient online submission
- thorough peer review by experienced researchers in your field
- rapid publication on acceptance
- support for research data, including large and complex data types
- gold Open Access which fosters wider collaboration and increased citations
- maximum visibility for your research: over 100M website views per year

At BMC, research is always in progress.

Learn more biomedcentral.com/submissions

